arXiv:2505.07015v1 [math.AP] 11 May 2025

RATE OF CONVERGENCE FOR A NONLOCAL-TO-LOCAL LIMIT IN ONE DIMENSION

JOSÉ A. CARRILLO, CHARLES ELBAR, STEFANO FRONZONI, AND JAKUB SKRZECZKOWSKI

Abstract. We consider a nonlocal approximation of the quadratic porous medium equation where the pressure is given by a convolution with a mollification kernel. It is known that when the kernel concentrates around the origin, the nonlocal equation converges to the local one. In one spatial dimension, for a particular choice of the kernel, and under mere assumptions on the initial condition, we quantify the rate of convergence in the 2-Wasserstein distance. Our proof is very simple, exploiting the so-called Evolutionary Variational Inequality for both the nonlocal and local equations as well as a priori estimates. We also present numerical simulations using the finite volume method, which suggests that the obtained rate can be improved - this will be addressed in a forthcoming work.

1. Introduction

We consider the nonlocal PDE

$$\partial_t u_\varepsilon - \partial_x(u_\varepsilon\, \partial_x W_\varepsilon * u_\varepsilon) = 0 \tag{1.1}$$

where $W_\varepsilon \approx \delta_0$ as $\varepsilon \to 0$. More precisely, we choose W_ε to satisfy $W_\varepsilon(x) = \frac{1}{\varepsilon} W\left(\frac{x}{\varepsilon}\right)$ where $W(x) = \frac{1}{2}e^{-|x|}$. It is well-known that W_ε satisfies the elliptic PDE

$$-\varepsilon^2 \partial_{xx} W_\varepsilon + W_\varepsilon = \delta_0. \tag{1.2}$$

It is known [13, 18] that solutions of (1.1) converge as $\varepsilon \to 0$ to the solution of

$$\partial_t u - \partial_x(u\, \partial_x u) = \partial_t u - \partial_{xx} \frac{u^2}{2} = 0. \tag{1.3}$$

2020 *Mathematics Subject Classification.* 35A15, 35Q70, 35B40, 65M08.

Key words and phrases. nonlocal equation, nonlocal-to-local limit, blob method, particle method, porous medium equation, evolutionary variational inequality, rate of convergence, finite volume method.

The nonlocal-to-local limit as above appears in several contexts. In mathematical biology, it connects models of tissue growth with so-called Brinkman's and Darcy's pressures as given by (1.1) and (1.3) respectively [13, 18]. This type of model has been studied in the context of their connection with the free boundary model of tumor growth [14, 16, 20, 22]. In numerical analysis, the nonlocal equation (1.1), viewed as a continuity equation, provides an approximation scheme, called the blob method, for solving (1.3). Starting from works of Oelschläger [21] and Lions-MasGallic [19], this approach has been extensively studied and generalized to more complicated equations and systems, including nonlinear porous medium equations [8, 10], cross-diffusion systems [5, 15], heat equation and fast-diffusion equations [9, 12].

The target of this paper is to provide a simple argument leading to the rate of convergence as $\varepsilon \to 0$ in the Wasserstein distance. In what follows, we write $\mathcal{P}_2(\mathbb{R})$ for the space of probability measures ρ such that $\int_{\mathbb{R}} \rho\, |x|^2 \,\mathrm{d}x < \infty$ and $\mathcal{W}_2$ for the second Wasserstein distance.

Theorem 1.1. *Let $u^0 \in \mathcal{P}_2(\mathbb{R}) \cap L^\infty(\mathbb{R})$. Let u_ε be the unique solution of* (1.1) *and let u be the unique solution of* (1.3) *with initial condition u^0. Then, there exists a constant $C = C(u^0, T, W)$ such that for all $t \in [0, T]$*

$$\mathcal{W}_2(u_\varepsilon(t,\cdot), u(t,\cdot)) \leq C\sqrt{\varepsilon}. \tag{1.4}$$

We present the proof in Section 2. The two main ingredients are a priori estimates for (1.1) and evolutionary variational inequality for both (1.1) and (1.3). In Section 3 we present numerical simulations obtained via finite volume method.

The recent paper [1] discusses the rate of convergence of the nonlocal-to-local limit in much broader generality. First, in one space dimension they are able to consider any kernel which is convex on $(-\infty, 0)$ and $(0, \infty)$ including our result. Second, they are able to establish the rate in higher dimensions. While it is true that [1] includes our result, the methods are substantially different and more complicated. The result of [1] is based on the well-known formula for the time derivative of the Wasserstein distance [25, Theorem 5.24] while our

work is based on the EVI formulation. The difference is also reflected by the assumptions on the initial datum: [1] needs u^0 to be in $W^{1,\infty}(\mathbb{T})$ (the paper discusses the problem on the torus $\mathbb{T}$) while we require $L^1(\mathbb{R}) \cap L^\infty(\mathbb{R})$ regularity (together with $u^0\,|x|^2 \in L^1(\mathbb{R})$). In particular, we do not make any assumptions on the derivatives of u^0.

It is natural to ask whether the rate $\sqrt{\varepsilon}$, also obtained in [1], is optimal. The numerical simulations presented in Figures 2 and 3 suggest that the rate could potentially be improved to ε for small values of ε. In a forthcoming work [6], we confirm that this is indeed the case. The result is based on a new formula for the Wasserstein distance between two gradient flows and on Aronson-Bénilan-type estimates for the porous medium equation.

2. Proof of Theorem 1.1

2.1. **Uniform estimates for nonlocal equation** (1.1)**.** In this section, for the sake of completeness, we briefly recall the following uniform bounds on (1.1) obtained in [23, 24].

Proposition 2.1. *Let $u^0 \in L^1(\mathbb{R}) \cap L^\infty(\mathbb{R})$, $u^0 \geq 0$, $u^0|x|^2 \in L^1(\mathbb{R})$. Then, there exists unique solution $\{u_\varepsilon\}$ to* (1.1) *with initial condition u^0 such that*

(A) $\{u_\varepsilon\}$ is uniformly bounded in $L^p((0,T)\times\mathbb{R})$ for all $p \in [1,\infty]$,
(B) $\{u_\varepsilon\,|\log(u_\varepsilon)|\}$, $\{u_\varepsilon\,|x|^2\}$ are uniformly bounded in $L^\infty(0,T;L^1(\mathbb{R}))$,
(C) $\{\partial_x W_\varepsilon * u_\varepsilon\}$ is uniformly bounded in $L^2((0,T)\times\mathbb{R})$,
(D) $\{\varepsilon\,\partial_{xx} W_\varepsilon * u_\varepsilon\}$ is uniformly bounded in $L^2((0,T)\times\mathbb{R})$,
(E) $\{\sqrt{u_\varepsilon}\,|\partial_x W_\varepsilon * u_\varepsilon|^2\}$ is uniformly bounded in $L^2((0,T)\times\mathbb{R})$.

Remark 2.2. The assumptions on the initial datum u^0 imply that $\int_\mathbb{R} u^0\,|\log u^0|\,\mathrm{d}x < \infty$. Indeed, one splits $\mathbb{R}$ for three sets $A_1 = \{x \in \mathbb{R} : u^0 > 1\}$, $A_2 = \{x \in \mathbb{R} : u^0 \leq e^{-|x|^2}\}$, $A_3 = \{x \in \mathbb{R} : e^{-|x|^2} < u^0 \leq 1\}$ so that

$$\int_\mathbb{R} u^0\,|\log u^0|\,\mathrm{d}x \leq \int_{A_1} u^0\,(u^0+1)\,\mathrm{d}x + \int_{A_2} e^{-|x|^2/2}\,\mathrm{d}x + \int_{A_3} u^0\,|x|^2\,\mathrm{d}x.$$

On the set A_2 we used that $|\sqrt{x}\,\log x| \leq 1$ for $0 \leq x \leq 1$.

Proof. The existence and uniqueness in one dimension is classical and can be proved either directly by a fixed point argument as in [17] or by using geodesic convexity of the energy

$E_\varepsilon[\rho] = \int_{\mathbb{R}} \rho * W_\varepsilon \, \rho \, \mathrm{d}x$ on $\mathcal{P}_2(\mathbb{R})$ equipped with the Wasserstein distance $\mathcal{W}_2$ cf. [3, Proposition 11.1.4]. Concerning the estimates, we first write (1.1) as

$$\partial_t u_\varepsilon - \partial_x u_\varepsilon \, \partial_x W_\varepsilon * u_\varepsilon - u_\varepsilon \, \partial_{xx} W_\varepsilon * u_\varepsilon = 0$$

so that using (1.2) we get

$$\partial_t u_\varepsilon = \partial_x u_\varepsilon \, \partial_x W_\varepsilon * u_\varepsilon - \frac{1}{\varepsilon^2}(u_\varepsilon - W_\varepsilon * u_\varepsilon).$$

Noting that in the point $x^* \in \mathbb{R}$ where $x \mapsto u_\varepsilon(t,x)$ reaches maximum we have $\partial_x u_\varepsilon(t,x^*) = 0$ and $u_\varepsilon - W_\varepsilon * u_\varepsilon \geq 0$ we obtain $\partial_t u_\varepsilon(x^*) \leq 0$ and this proves the claim. This argument comes from [26, Lemma 2.1].

The other estimates follow by usual energy considerations. Firstly, we multiply (1.1) by $W_\varepsilon * u_\varepsilon$ and we obtain

$$\partial_t \int_{\mathbb{R}^d} \frac{1}{2} u_\varepsilon W_\varepsilon * u_\varepsilon \, \mathrm{d}x + \int_{\mathbb{R}} u_\varepsilon |\partial_x (W_\varepsilon * u_\varepsilon)|^2 \, \mathrm{d}x. \tag{2.1}$$

Next, we multiply (1.1) with $|x|^2/2$ to get

$$\partial_t \frac{1}{2} \int_{\mathbb{R}} u_\varepsilon |x|^2 \, \mathrm{d}x = -\int_{\mathbb{R}} u_\varepsilon \, \partial_x (W_\varepsilon * u_\varepsilon) \, x \, \mathrm{d}x \leq \left(\int_{\mathbb{R}} u_\varepsilon |x|^2 \, \mathrm{d}x \right)^{1/2} \left(\int_{\mathbb{R}} u_\varepsilon |\partial_x W_\varepsilon * u_\varepsilon|^2 \, \mathrm{d}x \right)^{1/2},$$

so that using (2.1) and the Gronwall's inequality, we obtain a uniform bound on $\int_{\mathbb{R}} u_\varepsilon \, |x|^2 \, \mathrm{d}x$. Finally, multiplying (1.1) with $\log u_\varepsilon$ and using (1.2) we get

$$\partial_t \int_{\mathbb{R}} u_\varepsilon \log u_\varepsilon \, \mathrm{d}x + \int_{\mathbb{R}} |\partial_x W_\varepsilon * u_\varepsilon|^2 \, \mathrm{d}x + \varepsilon^2 \int_{\mathbb{R}} |\partial_{xx} W_\varepsilon * u_\varepsilon|^2 \, \mathrm{d}x = 0.$$

The negative part $\int_{\mathbb{R}} u_\varepsilon |\log u_\varepsilon|^- \, \mathrm{d}x$ is easily controlled by means of the moment estimate $\int_{\mathbb{R}} u_\varepsilon \, |x|^2 \, \mathrm{d}x$ as in Remark 2.2. The proof of Proposition 2.1 is concluded. □

2.2. **The theory of gradient flows.** We recall from [3, Theorem 11.1.4] the following result characterizing gradient flows on the space of probability measures $\mathcal{P}_2(\mathbb{R})$ equipped with the Wasserstein distance $\mathcal{W}_2$.

Theorem 2.3. *Let $F : \mathcal{P}_2(\mathbb{R}) \to (-\infty, +\infty]$ be a lower semicontinuous and λ-geodesically convex functional (on $(\mathcal{P}_2(\mathbb{R}), \mathcal{W}_2)$). For any $\mu_0 \in \mathcal{P}_2(\mathbb{R})$ there exists at most one gradient flow μ_t satisfying the initial condition μ_0 characterized by the evolutionary variational*

inequality

$$F(\mu_t) + \frac{1}{2}\frac{\mathrm{d}}{\mathrm{d}t}\mathcal{W}_2^2(\mu_t,\sigma) + \frac{\lambda}{2}\,\mathcal{W}_2^2(\mu_t,\sigma) \le F(\sigma) \tag{2.2}$$

which holds for a.e. t and $\sigma \in D(F)$ (the domain of F).

In the proof of Theorem 1.1 we apply Theorem 2.3 to two functionals

$$E[\rho] = \frac{1}{2}\int_{\mathbb{R}} \rho^2 \,\mathrm{d}x, \qquad\qquad E_\varepsilon[\rho] = \frac{1}{2}\int_{\mathbb{R}} W_\varepsilon * \rho\,\rho\,\mathrm{d}x.$$

Proposition 2.4. *The functionals E and E_ε are λ-geodesically convex on $(\mathcal{P}_2(\mathbb{R}),\mathcal{W}_2)$ with $\lambda = 0$.*

Proof. The functional E is well known to be geodesically convex cf. [28, Theorem 5.15]. Concerning E_ε, we follow the argument from [11, Proposition 2.7]. Consider ρ_0, $\rho_1 \in \mathcal{P}_2(\mathbb{R})$ and the geodesic $\rho_t = ((1-t)\,I + t\,T)\#\rho_0$ where I is the identity map while T is the optimal transport map between ρ_0 and ρ_1. We compute

$$E_\varepsilon[\rho_t] = \frac{1}{2}\int_{\mathbb{R}\times\mathbb{R}} W_\varepsilon((1-t)(x-y) + t(T(x)-T(y))\,\mathrm{d}\rho_0(x)\,\mathrm{d}\rho_0(y)$$

Then we can split the integral for the sets $x > y$ and $x \le y$. Since the transport map T in one dimension is monotone (so that $x > y$ implies $T(x) \ge T(y)$) and W is convex in $(-\infty, 0]$ and $[0, +\infty)$ we compute

$$\begin{aligned} E_\varepsilon[\rho_t] \le{}& \frac{(1-t)}{2}\int_{\mathbb{R}}\int_{x>y} W_\varepsilon(x-y)\,\mathrm{d}\rho_0(x)\,\mathrm{d}\rho_0(y) + \frac{t}{2}\int_{\mathbb{R}}\int_{x>y} W_\varepsilon(x-y)\,\mathrm{d}\rho_1(x)\,\mathrm{d}\rho_1(y) \\ &+ \frac{(1-t)}{2}\int_{\mathbb{R}}\int_{x\le y} W_\varepsilon(x-y)\,\mathrm{d}\rho_0(x)\,\mathrm{d}\rho_0(y) + \frac{t}{2}\int_{\mathbb{R}}\int_{x\le y} W_\varepsilon(x-y)\,\mathrm{d}\rho_1(x)\,\mathrm{d}\rho_1(y) \\ &= (1-t)E_\varepsilon[\rho_0] + tE_\varepsilon[\rho_1], \end{aligned}$$

so that E_ε is indeed geodesically convex. □

2.3. **Proof of Theorem 1.1.** The unique solutions of the EVI (2.2) in Theorem 2.3 with $F = E_\varepsilon$ and $F = E$ coincide with the unique solutions of u_ε, u of (1.1) and (1.3), see for instance [2, Proposition 3.28, Proposition 3.38]. By the EVI (2.2) for (1.1) we have

$$\frac{1}{2}\frac{\mathrm{d}}{\mathrm{d}t}\mathcal{W}_2^2(u_\varepsilon(t,\cdot),u(s,\cdot)) \le E_\varepsilon(u(s,\cdot)) - E_\varepsilon(u_\varepsilon(t,\cdot)). \tag{2.3}$$

Similarly, by the EVI (2.2) for (1.3)

$$\frac{1}{2}\frac{\mathrm{d}}{\mathrm{d}t}\mathcal{W}_2^2(u(t,\cdot),u_\varepsilon(s,\cdot)) \leq E(u_\varepsilon(s,\cdot)) - E(u(t,\cdot)). \tag{2.4}$$

Combining (2.3) and (2.4) we get

$$\frac{1}{2}\frac{\mathrm{d}}{\mathrm{d}t}\mathcal{W}_2^2(u_\varepsilon(t,\cdot),u(t,\cdot)) \leq E_\varepsilon(u(t,\cdot)) - E(u(t,\cdot)) + E(u_\varepsilon(t,\cdot)) - E_\varepsilon(u_\varepsilon(t,\cdot)).$$

By the inequality $u(x)\,u(y) \leq \frac{1}{2}u(x)^2 + \frac{1}{2}u(y)^2$ we have $E_\varepsilon(u(t,\cdot)) - E(u(t,\cdot)) \leq 0$. Therefore, it is sufficient to estimate $\int_0^T |E_\varepsilon(u_\varepsilon(t,\cdot)) - E(u_\varepsilon(t,\cdot))|\,\mathrm{d}t$. Clearly,

$$|E_\varepsilon(u_\varepsilon(t,\cdot)) - E(u_\varepsilon(t,\cdot))| = \frac{1}{2}\left|\int_{\mathbb{R}} u_\varepsilon\,(u_\varepsilon - u_\varepsilon * W_\varepsilon)\,\mathrm{d}x\right| \leq \frac{1}{2}\|u_\varepsilon\|_{L^2_x}\,\|u_\varepsilon - u_\varepsilon * W_\varepsilon\|_{L^2_x}.$$

Using the elliptic PDE (1.2), we write $u_\varepsilon - u_\varepsilon * W_\varepsilon = -\varepsilon^2\partial_{xx}u_\varepsilon * W_\varepsilon$ so that integrating in time and using (D) in Proposition 2.1

$$\int_0^T |E_\varepsilon(u_\varepsilon(t,\cdot)) - E(u_\varepsilon(t,\cdot))|\,\mathrm{d}t \leq \frac{1}{2}\|u_\varepsilon\|_{L^2_{t,x}}\,\|\varepsilon^2\partial_{xx}u_\varepsilon * W_\varepsilon\|_{L^2_{t,x}} \leq C\,\varepsilon.$$

The proof is concluded.

3. A Finite Volume scheme

We propose now a numerical scheme in one dimension, based on finite volumes, to analyse further the result of Theorem 1.1. We consider a one-dimensional domain $\Omega = (r_1, r_2)$ and we divide it into N cells of the form $[x_{i-\frac{1}{2}}, x_{i+\frac{1}{2}}]$, for $i = 1,\dots,N$, and for simplicity we assume that the cells have uniform size, that is $x_{i+\frac{1}{2}} - x_{i-\frac{1}{2}} = (r_2 - r_1)/N =: \Delta x$ for all $i = 1,\dots,N$. Each cell is centered at the points x_i, where $x_i = r_1 + (i/2)\Delta x$.

We denote by $\bar{u}^i_\varepsilon(t)$ the average of the solution $u_\varepsilon(x,t)$ over the i-th cell:

$$\bar{u}^i_\varepsilon(t) = \frac{1}{\Delta x}\int_{C_i} u_\varepsilon(t,x)\,\mathrm{d}x.$$

If we now integrate equation (1.1) on each cell C_i we have a system of differential equations, given by

$$\frac{d\bar{u}^i_\varepsilon}{dt} = \frac{F(u_\varepsilon(t,x_{i+\frac{1}{2}})) - F(u_\varepsilon(t,x_{i-\frac{1}{2}}))}{\Delta x}, \quad i = 1,\dots,N \tag{3.1a}$$

where the flux F is given by $F(u_\varepsilon) := u_\varepsilon\,\partial_x W_\varepsilon * u_\varepsilon$.

We then approximate the flux at the cell interface with functions $F_{i+\frac{1}{2}}$ and $F_{i-\frac{1}{2}}$ approximating respectively $F(u_\varepsilon(t, x_{i+\frac{1}{2}}))$ and $F(u_\varepsilon(t, x_{i-\frac{1}{2}}))$. For constructing these approximations we use upwinding in a standard way for which the reader can refer to [4, 7]:

$$F_{i+\frac{1}{2}} = v^+_{i+\frac{1}{2}}(u^i_\varepsilon)^{\mathrm{R}} + v^-_{i-\frac{1}{2}}(u^i_\varepsilon)^{\mathrm{L}}, \tag{3.1b}$$

where

$$v_{i+\frac{1}{2}} = \frac{W_\varepsilon * u_\varepsilon(x_{i+1}) - W_\varepsilon * u_\varepsilon(x_i)}{\Delta x}, \quad v^+_{i+\frac{1}{2}} = \max(v_{i+\frac{1}{2}}, 0), \quad v^-_{i+\frac{1}{2}} = \min(v_{i+\frac{1}{2}}, 0).$$

A corresponding expression holds for $F_{i-\frac{1}{2}}$.

For the values of $(u^i_\varepsilon)^{\mathrm{R}}$ and $(u^i_\varepsilon)^{\mathrm{L}}$ we can choose a first or second order approximation. We can define

$$\tilde{u_\varepsilon}(x) = \bar{u}^i_\varepsilon + (u_\varepsilon)^i_x(x - x_i) \quad \text{for } x \in [x_{i-\frac{1}{2}}, x_{i+\frac{1}{2}}]$$

and we would have

$$(u^i_\varepsilon)^{\mathrm{R}} = \bar{u}^i_\varepsilon + \frac{\Delta x}{2}(u_\varepsilon)^i_x, \qquad (u^i_\varepsilon)^{\mathrm{L}} = \bar{u}^i_\varepsilon - \frac{\Delta x}{2}(u_\varepsilon)^i_x.$$

If one sets $(u_\varepsilon)^i_x = 0$ for all $i = 1, \dots, N$, we have a first order approximation, while if we consider a piecewise linear approximation, the scheme is second order accurate in space by imposing nonnegativity of the density reconstruction. With this purpose, we can make a choice for a non-vanishing numerical slope limiter guaranteeing that the reconstructed point values are nonnegative as long as the values of the solution are nonnegative. We can use a generalized minmod limiter

$$(u_\varepsilon)^i_x = \mathrm{minmod}\left(\theta\frac{\bar{u}^{i+1}_\varepsilon - \bar{u}^i_\varepsilon}{\Delta x}, \frac{\bar{u}^{i+1}_\varepsilon - \bar{u}^{i-1}_\varepsilon}{2\Delta x}, \theta\frac{\bar{u}^i_\varepsilon - \bar{u}^{i-1}_\varepsilon}{\Delta x}\right),$$

where the parameter θ controls numerical viscosity and

$$\mathrm{minmod}(a, b, c) := \begin{cases} \min\{a, b, c\} & \text{if } a, b, c > 0, \\ \max\{a, b, c\} & \text{if } a, b, c < 0, \\ 0 & \text{otherwise.} \end{cases} \tag{3.2}$$

The term $W_\varepsilon * u_\varepsilon(x_i)$ is approximated as a linear combination

$$W_\varepsilon * u_\varepsilon(x_i) = \sum_{j=1}^{N}\left(\int_{x_{j-\frac{1}{2}}}^{x_{j+\frac{1}{2}}} \frac{1}{2\varepsilon}e^{-\frac{|x_i - y|}{\varepsilon}}\mathrm{d}y\right)\overline{u}^j_\varepsilon = (\mathcal{I}\overline{u}_\varepsilon)_i, \tag{3.3}$$

where $\mathcal{I} \in \mathbb{R}^{N\times N}$ is the matrix

$$\mathcal{I} = \begin{pmatrix} I_1(x_1) & I_2(x_1) & \dots & I_N(x_1) \\ I_1(x_2) & I_2(x_2) & \dots & I_N(x_2) \\ \vdots & \vdots & \ddots & \vdots \\ I_1(x_N) & I_2(x_N) & \dots & I_N(x_N) \end{pmatrix}, \tag{3.4}$$

with

$$I_j(x_i) = \int_{x_{j-\frac{1}{2}}}^{x_{j+\frac{1}{2}}} \frac{1}{2\varepsilon} e^{-\frac{|x_i-y|}{\varepsilon}} \mathrm{d}y. \tag{3.5}$$

Moreover, the above term can be explicitly computed as

$$I_j(x_i) = \begin{cases} \frac{1}{2}\Big(e^{\frac{x_i-x_{j-\frac{1}{2}}}{\varepsilon}} - e^{\frac{x_i-x_{j+\frac{1}{2}}}{\varepsilon}}\Big) & \text{if } x_{j-\frac{1}{2}} > x_i, \\ \frac{1}{2}\Big(e^{-\frac{x_i-x_{j+\frac{1}{2}}}{\varepsilon}} - e^{-\frac{x_i-x_{j-\frac{1}{2}}}{\varepsilon}}\Big) & \text{if } x_{j+\frac{1}{2}} < x_i, \\ 1 - e^{-\frac{\Delta x}{2\varepsilon}} & \text{if } i = j. \end{cases}$$

Remark 3.1. Notice that for fixed Δx as $\varepsilon \to 0$ the matrix $\mathcal{I}$ tends to the identity matrix, making the scheme converging to the scheme of the standard porous medium equation with exponent 2. Therefore, from the numerical point of view, we recover the switch from nonlocal (for larger values of ε giving a full matrix $\mathcal{I}$) to local (for ε approaching zero, the sparsity of $\mathcal{I}$ increases up to reaching the identity).

Remark 3.2. The scheme (3.1) has to be paired with some boundary conditions. In our experiments we will use either a no-flux boundary condition or a periodic boundary condition. The no-flux boundary condition imposes a vanishing flux at the endpoints of the one-dimensional domain $F_{i-\frac{1}{2}} = F_{N+\frac{1}{2}} = 0$, while the periodic boundary condition imposes $F_{i-\frac{1}{2}} = F_{N+\frac{1}{2}}$. We will see later that the choice of the type of boundary condition is crucial for the rate of convergence in ε.

Remark 3.3. In our numerical experiments, in addition to the finite volume scheme, that we have summarised above for equation (1.1), we will also consider a finite volume scheme to the self-similar Fokker-Planck equation, associated to it. In particular we will consider the Fokker-Planck equation

$$\partial_t u - \partial_x(u\,\partial_x u) - \partial_x(xu) = 0, \tag{3.6}$$

together with its nonlocal approximation, given by

$$\partial_t u_\varepsilon - \partial_x(u_\varepsilon \partial_x W_\varepsilon * u_\varepsilon) - \partial_x(x u_\varepsilon) = 0. \tag{3.7}$$

The numerical scheme for (3.7) can be easily written as (3.1), where the flux terms $F_{i\pm\frac{1}{2}}$ includes an additional term, that takes into account the source of flux due to the Fokker-Planck term $\partial_x(x u_\varepsilon)$, see [7] for further details.

Remark 3.4. A consideration on the relationship between Δx and ε has to be made. In fact we will use the scheme to check the order of convergence in estimate (1.4). In order to get numerically the correct order of convergence for ε small, one should pick the size of the cells smaller or at least equal to the value of ε: $\Delta x \leq \varepsilon$. The intuition behind this requirement is sketched in Figure 1. The parameter ε controls the level of nonlocal interaction in equation (1.1) and as it decreases towards zero the non-locality diminishes its range, meaning that (1.1) approaches the local problem (1.3). Therefore, for smaller values of ε, to ensure that we still detect the nonlocal interactions through the finite volume scheme (3.1), the size of the cells must have at least the same size of ε.

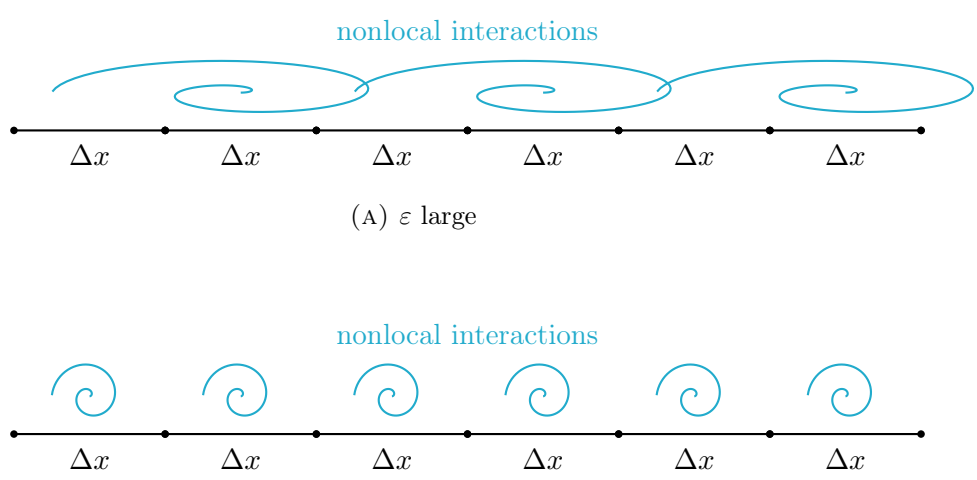

(A) ε large

(B) ε small

FIGURE 1. Finite Volume scheme: size of cells and ε

4. Numerical experiments

We use the scheme (3.1) to analyse the estimate of Theorem 1.1. The scheme is implemented on one-dimensional domains with varying initial and boundary conditions, allowing us to investigate various aspects of convergence as well as the properties of the equation (1.1). In the following, we will denote by u_0 the solution u of the local models (1.3) and (3.6).

4.1. **Sharpness of the error estimate between the local and the nonlocal problem.** In Figure 2 we report for different times the convergence results in Wasserstein distance $\mathcal{W}_2$ between the numerical approximations of u_0 and u_ε, solutions of (1.3) and (1.1) respectively, using the finite volume scheme (3.1). The simulations in Figure 2 for different values of ε start all with a Gaussian initial datum $u^0 = \frac{1}{\sqrt{2\pi}} e^{-|x|^2/2}$. These experiments should resemble the behaviour of the equations on the whole of $\mathbb{R}$. The convergence plot validates the result of Theorem 1.1. In particular, we first observe that the estimate, provided by (1.4), is global in ε, meaning its proof imposes no restrictions on the values of ε. Figure 2 shows how the rate of convergence for $\mathcal{W}_2(u_\varepsilon, u_0)$, with this specific initial datum, is linear in ε for small values of ε, while for larger values of ε there is a transition and the convergence deteriorates behaving more like ε^β for $\beta < 1/4$. We have clearly that $\varepsilon < \sqrt{\varepsilon} < \varepsilon^{\frac{1}{4}}$ for $\varepsilon < 1$, and $\varepsilon^\beta < \varepsilon^{\frac{1}{4}} < \sqrt{\varepsilon} < \varepsilon$ for $\varepsilon > 1$. Therefore, the numerical results provided by our finite volume scheme demonstrate that the estimate of (1.4) is in fact the best, *global* in ε estimate, while the rate of ε from [6] is valid for small values of ε.

4.2. **Periodic boundary conditions.** In Figure 3, we test the case of periodic boundary conditions, starting from a compactly supported initial datum, $u^0 = (1 - |x|^2)_+$. The experiment resembles the behaviour that equation (1.1) has on the whole of $\mathbb{R}$ while the support does not touch the boundary of the domain. Once the support reaches the boundary we see the expected behavior converging towards the constant solution. We observe the expected rate of convergence for $\mathcal{W}_2(u_\varepsilon, u_0)$, similar to the experiments of Figure 2 during the whole evolution despite the periodic boundary conditions. The order of convergence remains indeed linear in ε for small values of ε for all times of the simulation. These numerical experiments corroborate again the results obtained in [6].

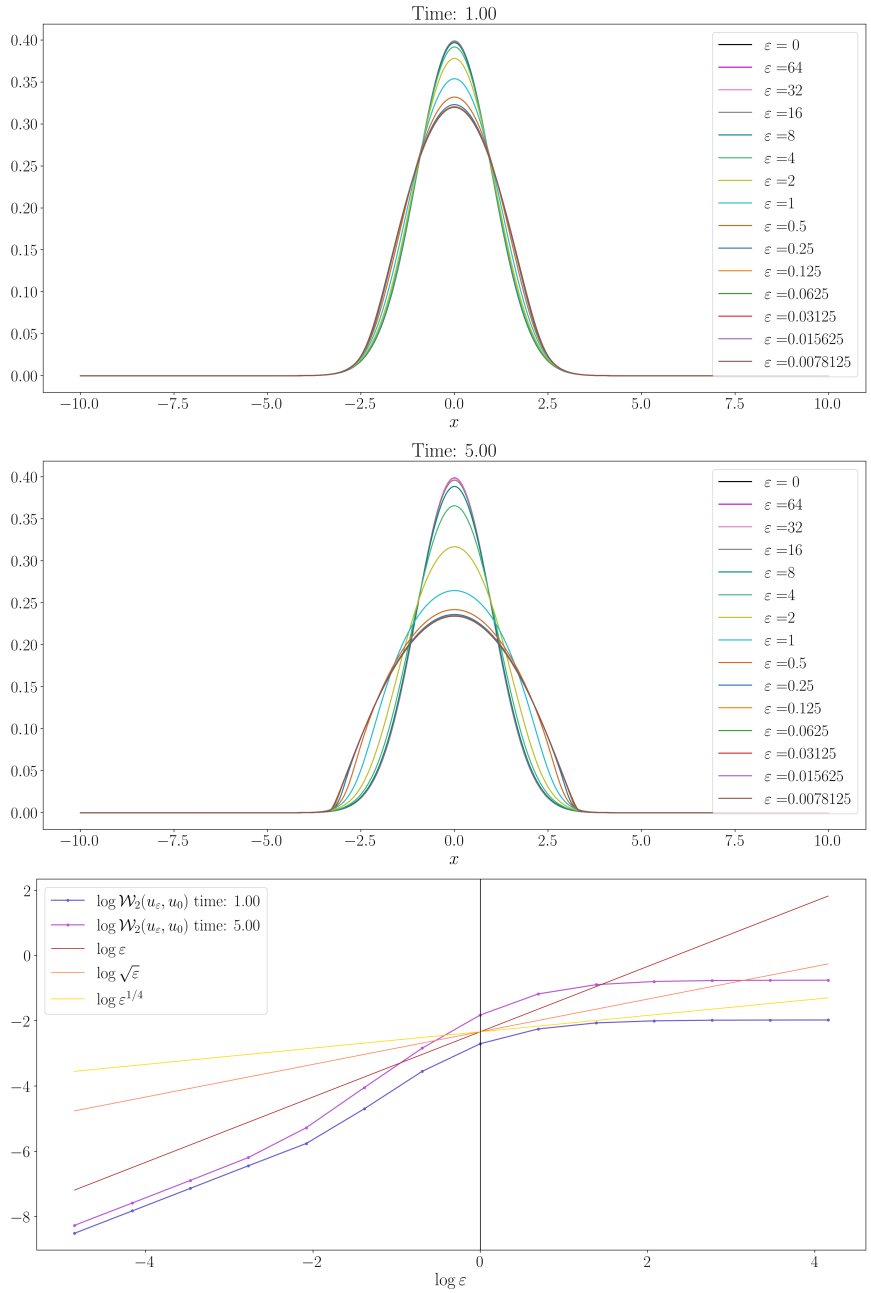

FIGURE 2. Porous medium equation versus blob method: order of convergence for $\mathcal{W}_2(u_\varepsilon, u_0)$, u_0 solution of (1.3) and u_ε solution of (1.1). The computational domain is $\Omega = (-10, 10)$, $u^0(x) = (1/\sqrt{2\pi})\exp(-|x|^2/2)$ is the initial datum, a uniform grid of $N = 2^{12}$ cells was used with $\Delta t = 0.01$.

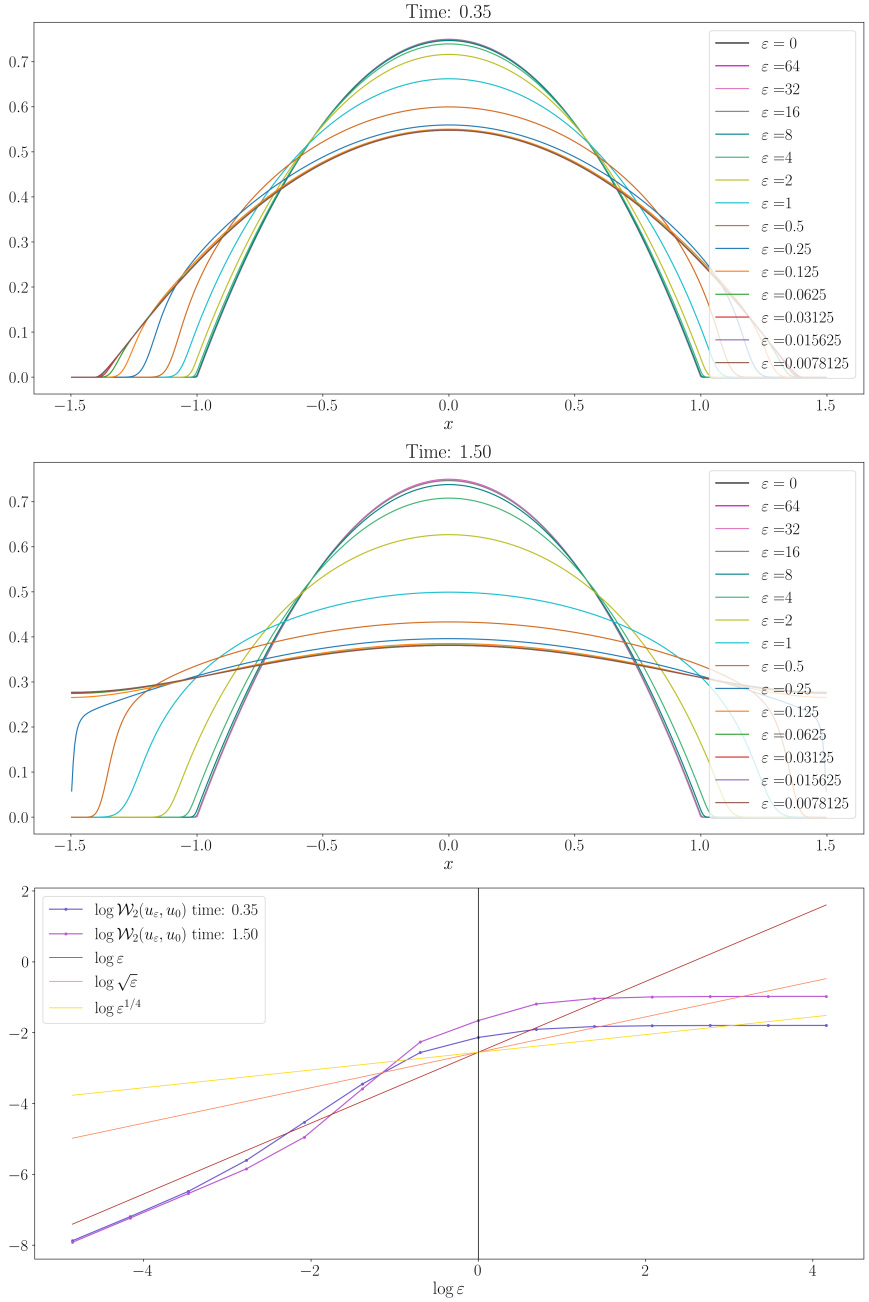

FIGURE 3. Porous medium equation and blob method: order of convergence for $\mathcal{W}_2(u_\varepsilon, u_0)$, u_0 solution of (1.3) and u_ε solution of (1.1). The computational domain $\Omega = (-3, 3)$, $u^0(x) = (1 - x^2)_+$ is the initial datum, a uniform grid of $N = 2^{10}$ cells with $\Delta t = 0.01$ was used, periodic boundary conditions were imposed.

4.3. **No flux boundary conditions.** In Figure 4 we test on a bounded domain the influence of the boundary on the convergence rate for $\mathcal{W}_2(u_\varepsilon, u_0)$, where u_0 and u_ε solve respectively (1.3) and (1.1). Starting from the same compactly supported initial datum, that we used in the experiments in Figure 3, we observe how the order of convergence for ε small is clearly linear in ε initially, as Figure 4 displays. However, after the solutions touch the boundary, and the density starts to accumulate at the boundary, one can observe a decrease of the order of convergence, that becomes approximately proportional to $\sqrt{\varepsilon}$, as reported in Figure 4. This experiment empirically highlights how the order of convergence may vary with respect to the case of the whole space, precisely due to the presence of the no-flux boundary conditions in contrast to [6], and how the interaction with the boundary might generally slow down convergence. In addition, we can notice how, imposing no-flux boundary conditions, lead to the accumulation of the density at the boundary points because the repulsive kernel pushes the density to concentrate at the boundary. The final steady states for u_ε get closer to the constant function as $\varepsilon \to 0$, except for the two boundary spikes, as one can observe in Figure 4 for intermediate times.

4.4. **Fokker-Planck problem and the effect of a bounded domain.** In Figure 5 we check the convergence for the analogous Fokker-Planck problem (3.7). All the simulations start in this case from a uniform distribution $u^0 = \frac{1}{|\Omega|} + 10$. Despite the support of the initial datum being the whole bounded domain Ω, the evolution converges towards the expected stationary state of the Fokker-Planck equation on the whole of $\mathbb{R}$ emulating the behavior on the whole line. We can still observe how the convergence follows a rate proportional ε^β with $\beta < 1/4$ for $\varepsilon \gg 1$, while, in particular for small times, the convergence for $\varepsilon \ll 1$ follows a rate of $\sqrt{\varepsilon}$, with a transition, where it becomes almost linear for ε close to 1. For larger times the behaviour of $\mathcal{W}_2(u_\varepsilon, u_0)$ seems to improve in terms of convergence, keeping however $\sqrt{\varepsilon}$ as convergence rate for the smallest values. This experiment not only validates the estimate (1.4), but it also show how the estimate is actually sharp for some initial data. The interaction with the boundary and the boundedness of the domain turns then to be decisive for obtaining the rate $\sqrt{\varepsilon}$, as in the previous subsection.

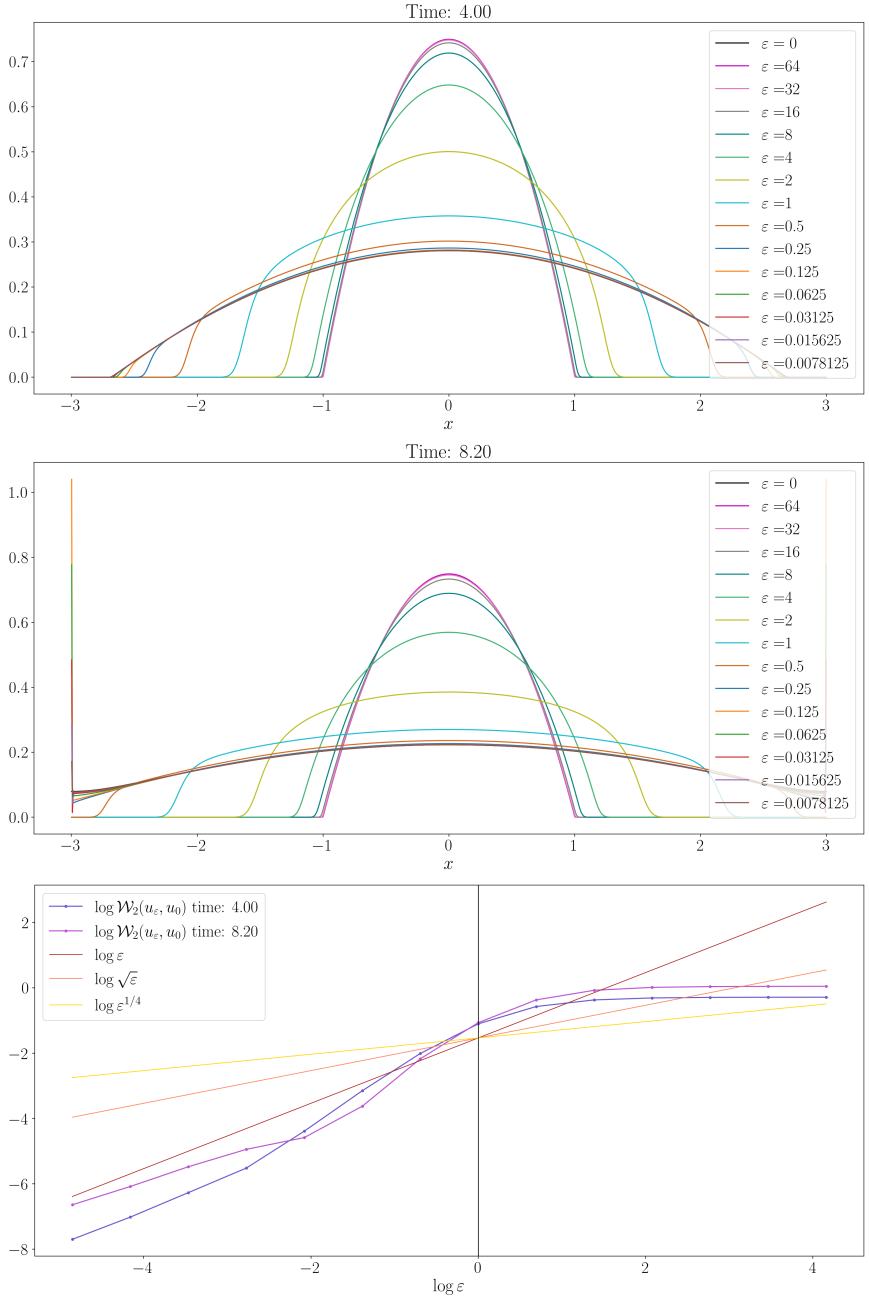

FIGURE 4. Porous medium equation and blob method: order of convergence for $\mathcal{W}_2(u_\varepsilon, u_0)$, u_0 solution of (1.3) and u_ε solution of (1.1). The computational domain is $\Omega = (-3, 3)$, $u^0(x) = (1 - x^2)_+$ is the initial datum, a uniform grid of $N = 2^{10}$ cells was used with $\Delta t = 0.01$, no-flux boundary conditions were imposed.

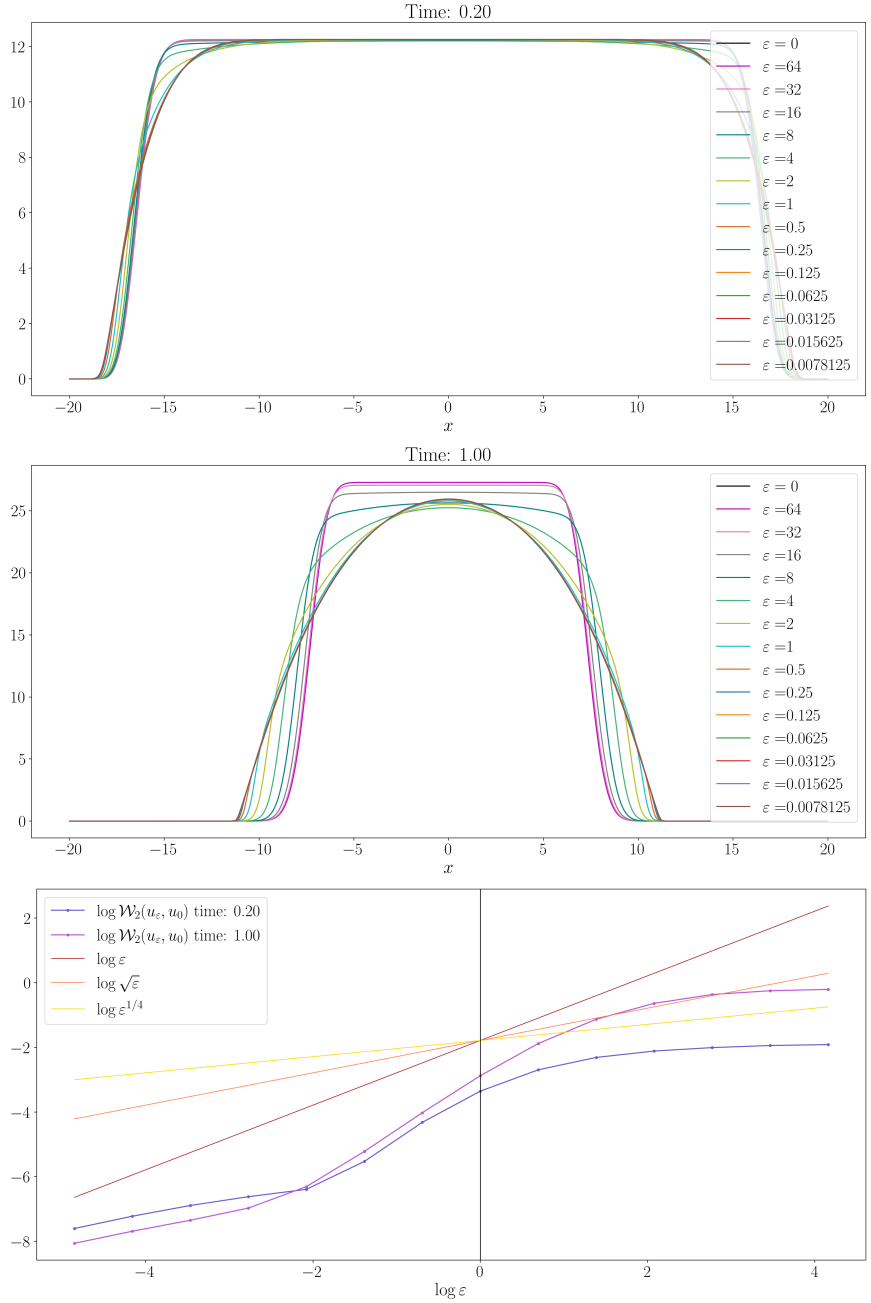

FIGURE 5. Porous medium Fokker-Planck equation and blob method: order of convergence for $\mathcal{W}_2(u_\varepsilon, u_0)$, u_0 solution of (3.6) and u_ε solution of (3.7). The computational domain is $\Omega = (-20, 20)$, $u^0(x) = 1/|\Omega| + 10$ is the initial datum, a uniform grid of $N = 2^{13}$ cells was used with $\Delta t = 0.01$.

Appendix A. Complementary material

A.1. **Nonlocal and local models: acquisition of regularity.** In Figure 6 we have the results for an interesting case, in which we consider an initial datum u^0, that is randomly generated and piecewise constant, with different values in each cell of the domain Ω. We can see in Figure 6 the same convergence behaviour previously observed: the Wasserstein distance $\mathcal{W}_2$ between u_0 and u_ε initially decreases like $\sqrt{\varepsilon}$ for small values of ε, with convergence slowing down for $\varepsilon \gg 1$. As time increases, the convergence becomes faster for $\varepsilon \ll 1$, as reported in Figure 6.

In addition in Figure 7 we can test a property that holds true for the porous medium equation: starting from an initial datum $u^0(x) = u(x,0) \in L^1(\mathbb{R}) \cap L^\infty(\mathbb{R})$, the solution $u_0(x,t)$ becomes immediately Hölder regular for $t > 0$ (the reader can refer to [25, 27] for more information on this property). This is not the case for the solution $u_\varepsilon(x,t)$ of the nonlocal approximation: while the solution remains in $L^1(\mathbb{R}) \cap L^\infty(\mathbb{R})$, it does not acquire the same regularity as u_0 as time progresses. This fact could be noticed also in Figure 6, where we can observe that u_ε does not gain regularity for larger values of u_ε in the center of the domain, where the density is driven by the Fokker-Planck term.

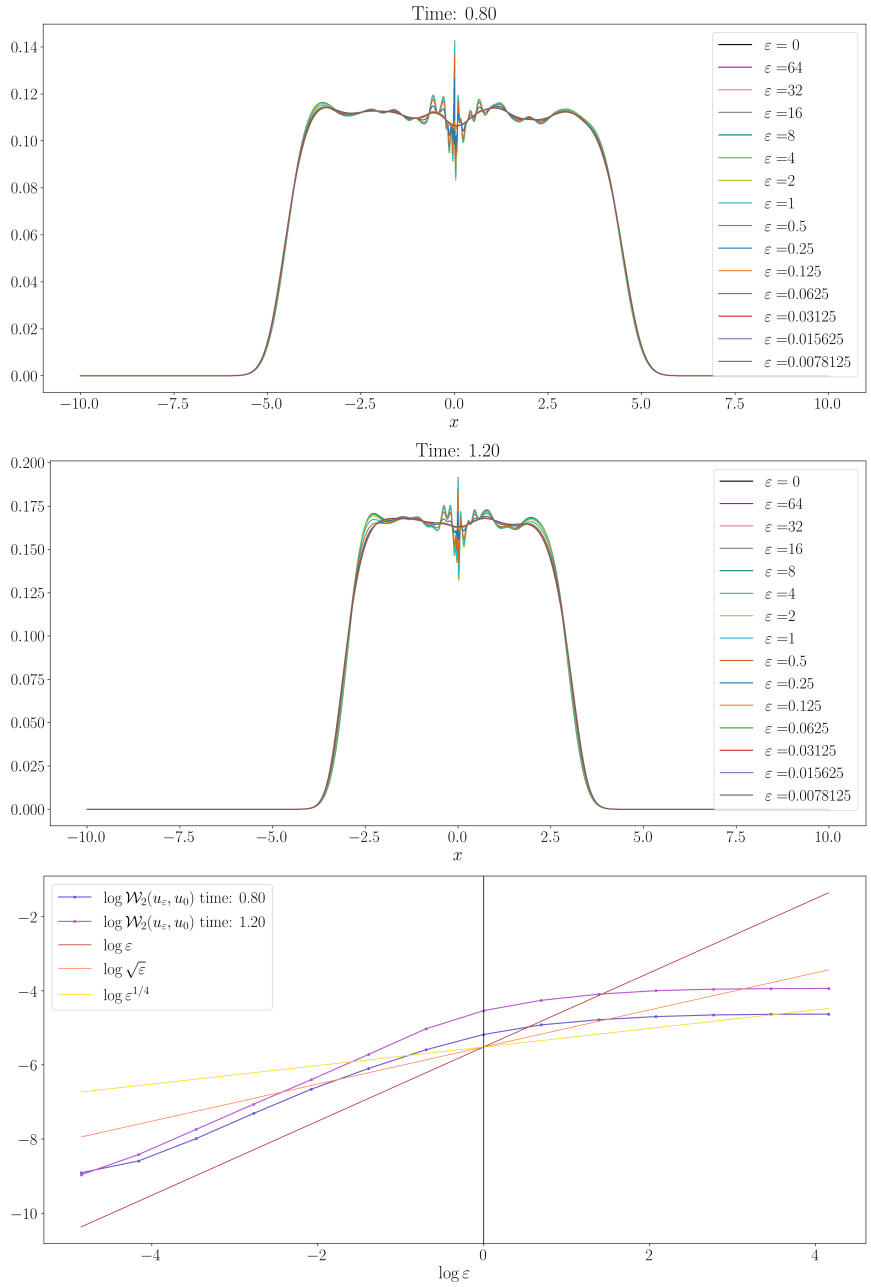

FIGURE 6. Porous medium equation and blob method: order of convergence for $\mathcal{W}_2(u_\varepsilon, u_0)$, u_0 (solution of (3.6)) and u_ε (solution of (3.7)). The computational domain is $\Omega = (-10, 10)$, $u^0(x) = u(x, 0)$, the initial datum, is generated using random values on a uniform grid of $N = 2^{12}$ cells, with $\Delta t = 0.01$.

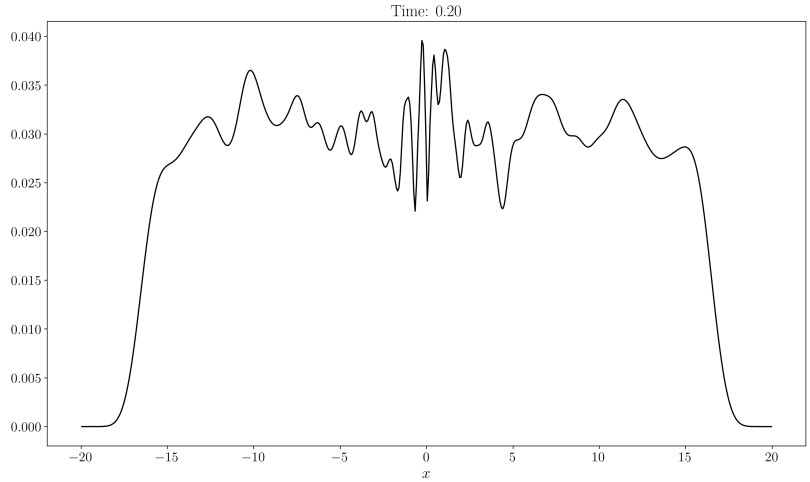

(A) $\varepsilon = 0$

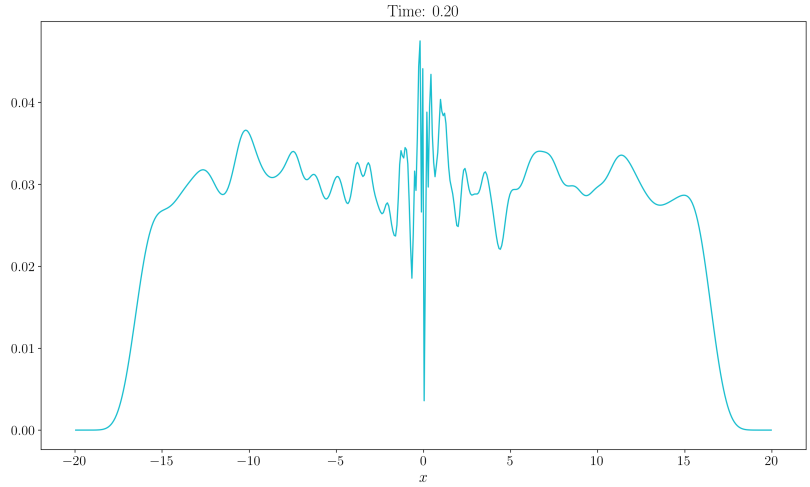

(B) $\varepsilon = 1$

FIGURE 7. Porous medium equation and blob method: u (solution of (3.6)) and u_ε (solution of (3.7)) for $\varepsilon = 1$. $\Omega = (-20, 20)$, $u^0(x) = u(x, 0)$ initial datum generated using random values on a uniform grid of $N = 2^9$ cells, $\Delta t = 0.01$.

Acknowledgements

This work was supported by the Advanced Grant Nonlocal-CPD (Nonlocal PDEs for Complex Particle Dynamics: Phase Transitions, Patterns and Synchronization) of the European Research Council Executive Agency (ERC) under the European Union's Horizon 2020 research and innovation programme (grant agreement No. 883363). JAC was also partially supported by the EPSRC grant numbers EP/T022132/1 and EP/V051121/1. CE was supported by the ERC AdG 101054420 EYAWKAJKOS project.

References

[1] A. Amassad and D. Zhou. A deterministic particle method for the porous media equation. *arXiv preprint arXiv:2501.18745*, 2025.

[2] L. Ambrosio and N. Gigli. A user's guide to optimal transport. In *Modelling and optimisation of flows on networks*, volume 2062 of *Lecture Notes in Math.*, pages 1–155. Springer, Heidelberg, 2013.

[3] L. Ambrosio, N. Gigli, and G. Savaré. *Gradient flows in metric spaces and in the space of probability measures*. Lectures in Mathematics ETH Zürich. Birkhäuser Verlag, Basel, second edition, 2008.

[4] R. Bailo, J. A. Carrillo, S. Fronzoni, and D. Gómez-Castro. A finite-volume scheme for fractional diffusion on bounded domains. *European Journal of Applied Mathematics*, page 1–21, 2024.

[5] M. Burger and A. Esposito. Porous medium equation and cross-diffusion systems as limit of nonlocal interaction. *Nonlinear Anal.*, 235:Paper No. 113347, 30, 2023.

[6] J. Carrillo, P. Gwiazda, and J. Skrzeczkowski. A new semigroup formula for the Wasserstein distance between two Wasserstein gradient flows. *In preparation*, 2025.

[7] J. A. Carrillo, A. Chertock, and Y. Huang. A finite-volume method for nonlinear nonlocal equations with a gradient flow structure. *Commun. Comput. Phys.*, 17(1):233–258, 2015.

[8] J. A. Carrillo, K. Craig, and F. S. Patacchini. A blob method for diffusion. *Calc. Var. Partial Differential Equations*, 58(2):Paper No. 53, 53, 2019.

[9] J. A. Carrillo, A. Esposito, J. Skrzeczkowski, and J. S.-H. Wu. Nonlocal particle approximation for linear and fast diffusion equations. *arXiv preprint arXiv:2408.02345*, 2024.

[10] J. A. Carrillo, A. Esposito, and J. S.-H. Wu. Nonlocal approximation of nonlinear diffusion equations. *Calc. Var. Partial Differential Equations*, 63(4):Paper No. 100, 44, 2024.

[11] J. A. Carrillo, L. C. F. Ferreira, and J. C. Precioso. A mass-transportation approach to a one dimensional fluid mechanics model with nonlocal velocity. *Adv. Math.*, 231(1):306–327, 2012.

[12] K. Craig, M. Jacobs, and O. Turanova. Nonlocal approximation of slow and fast diffusion. *J. Differential Equations*, 426:782–852, 2025.

[13] N. David, T. Dębiec, M. Mandal, and M. Schmidtchen. A degenerate cross-diffusion system as the inviscid limit of a nonlocal tissue growth model. *SIAM J. Math. Anal.*, 56(2):2090–2114, 2024.

[14] N. David and B. Perthame. Free boundary limit of a tumor growth model with nutrient. *J. Math. Pures Appl. (9)*, 155:62–82, 2021.

[15] M. Doumic, S. Hecht, B. Perthame, and D. Peurichard. Multispecies cross-diffusions: from a nonlocal mean-field to a porous medium system without self-diffusion. *J. Differential Equations*, 389:228–256, 2024.

[16] T. Dębiec, B. Perthame, M. Schmidtchen, and N. Vauchelet. Incompressible limit for a two-species model with coupling through Brinkman's law in any dimension. *J. Math. Pures Appl. (9)*, 145:204–239, 2021.

[17] T. Dębiec and M. Schmidtchen. Incompressible limit for a two-species tumour model with coupling through Brinkman's law in one dimension. *Acta Appl. Math.*, 169:593–611, 2020.

[18] C. Elbar and J. Skrzeczkowski. On the inviscid limit connecting Brinkman's and Darcy's models of tissue growth with nonlinear pressure. *J. Math. Fluid Mech.*, 27(2):Paper No. 28, 14, 2025.

[19] P.-L. Lions and S. Mas-Gallic. Une méthode particulaire déterministe pour des équations diffusives non linéaires. *C. R. Acad. Sci. Paris Sér. I Math.*, 332(4):369–376, 2001.

[20] A. Mellet, B. Perthame, and F. Quirós. A Hele-Shaw problem for tumor growth. *J. Funct. Anal.*, 273(10):3061–3093, 2017.

[21] K. Oelschläger. Large systems of interacting particles and the porous medium equation. *J. Differential Equations*, 88(2):294–346, 1990.

[22] B. Perthame, F. Quirós, and J. L. Vázquez. The Hele-Shaw asymptotics for mechanical models of tumor growth. *Arch. Ration. Mech. Anal.*, 212(1):93–127, 2014.

[23] B. Perthame, M. Tang, and N. Vauchelet. Traveling wave solution of the Hele-Shaw model of tumor growth with nutrient. *Math. Models Methods Appl. Sci.*, 24(13):2601–2626, 2014.

[24] B. Perthame and N. Vauchelet. Incompressible limit of a mechanical model of tumour growth with viscosity. *Philos. Trans. Roy. Soc. A*, 373(2050):20140283, 16, 2015.

[25] F. Santambrogio. *Optimal transport for applied mathematicians*, volume 87 of *Progress in Nonlinear Differential Equations and their Applications*. Birkhäuser/Springer, Cham, 2015. Calculus of variations, PDEs, and modeling.

[26] M. Tang, N. Vauchelet, I. Cheddadi, I. Vignon-Clementel, D. Drasdo, and B. Perthame. Composite waves for a cell population system modeling tumor growth and invasion. *Chinese Ann. Math. Ser. B*, 34(2):295–318, 2013.

[27] J. M. Urbano. *The method of intrinsic scaling*, volume 1930 of *Lecture Notes in Mathematics*. Springer-Verlag, Berlin, 2008. A systematic approach to regularity for degenerate and singular PDEs.

[28] C. Villani. *Topics in optimal transportation*, volume 58 of *Graduate Studies in Mathematics*. American Mathematical Society, Providence, RI, 2003.

José A. Carrillo: Mathematical Institute, University of Oxford, Woodstock Road, Oxford, OX2 6GG, United Kingdom

Email address: carrillo@maths.ox.ac.uk

Charles Elbar: Université Claude Bernard Lyon 1, ICJ UMR5208, CNRS, Ecole Centrale de Lyon, INSA Lyon, Université Jean Monnet, 69622 Villeurbanne, France

Email address: elbar@math.univ-lyon1.fr

Stefano Fronzoni: Mathematical Institute, University of Oxford, Woodstock Road, Oxford, OX2 6GG, United Kingdom

Email address: fronzoni@maths.ox.ac.uk

Jakub Skrzeczkowski: Mathematical Institute, University of Oxford, Woodstock Road, Oxford, OX2 6GG, United Kingdom

Email address: jakub.skrzeczkowski@maths.ox.ac.uk